RSC Advances

ROYAL SOCIETY OF CHEMISTRY

www.rsc.org/advances

Nitrogen-induced Ferromagnetism in BaO

Gul Rahman*

Department of Physics, Quaid-i-Azam University, Islamabad 45320, Pakistan

Abstract

Density functional theory with local spin density approximation is used to propose possible room temperature ferromagnetism in N-doped NaCl-type BaO. Pristine BaO is found to be a wide bandgap semiconductor, however, N induces large density of states at the Fermi level in the nonmagnetic state, which suggests magnetic instability within the Stoner mean field model. The spin-polarized calculations show that N-doped BaO is a true half- metal, and N has a large magnetic moment, which is mainly localized around the N atoms and a small polarization at the O sites is also observed. The origin of magnetism is linked with the electronic structure. The ferromagnetic(FM) and antiferromagnetic (AFM) coupling between the N atoms in BaO reveal that N-doped has a FM ground state, and the calculated transition temperature (T_C), within the Heisenberg mean field theory, theorizes possible room temperature FM in N-doped BaO. Nitrogen also induces ferromagnetism when doped at surface O site and has a smaller defect formation energy than the bulk N-doped BaO. The magnetism of N-doped BaO is also compared with Co-doped BaO, and we believe that N has good opportunities in tuning magnetism in BaO than Co in BaO.

I. INTRODUCTION

Inducing magnetism in non-magnetic oxides is one of the main areas of interest in the research community. Generally, many oxides are insulator and non-magnetic without magnetic impurity atoms, however, recent theoretical and experimental understanding of oxides can show ferromagnetism with defects or light elements, e.g., C, N, Li.[1–9] In the past decade, density functional theory (DFT) has played a vital role in either proposing new magnetic materials or elucidating the origins of defects-driven magnetism in oxides.[3–5,10–16] To date, there are few oxides that can show room temperature (RT) ferromagnetism, e.g., ZnO, SnO_2, In_2O_3, CeO_2.[13,17–19] Light elements are not only used to develop magnetism in oxides, but can also be used to stabilize intrinsic defects in the host materials.[20,21] In the combined efforts of theoreticians and experimentalists, we can believe in magnetism in oxides induced by non-magnetic impurities.[6,7,22,23] Now it is known that magnetism develops in the non-magnetic oxides where impurity atom has a finite local magnetic moment and this local magnetic moment will interact with each other to form a net magnetic moment in the host material. Those materials in which magnetism is induced by doping nonmagnetic impurities, the substitutional atom can have a finite magnetic moment and the $2p$-electrons of the doped atom plays an essential role in governing magnetism in the host material, are generally considered as d^0 magnetic materials. These nonmagnetic impurity atoms can also form impurity bands in the bandgap of host material, and ferromagnetic behavior can be expected if the Fermi energy lies in these impurity bands.

BaO is another oxide having interesting structural and electronic properties. It can be used as a NO_3 storage device for catalysis.[24] BaO is also considered as a precursor to the well known ferroelectric perovskite oxide $BaTiO_3$, which can have either TiO_2 or BaO terminated surface when $BaTiO_3$ is grown on a suitable substrate as a thin film. TiO_2 has been extensively studied for possible magnetism in TiO_2.[7] However, less attention has been given to impurities in BaO and there are no detailed theoretical and experimental studies on inducing magnetism in it. It is experimentally observed that bulk BaO naturally occurs in a B1 (NaCl) structure.[25] Recent experimental reports claim the grown of ultrathin BaO films on $SrTiO_3(001)$ substrate, and the formation of BaO nanoparticles on reconstructed $SrTiO_3(001)$, while a locally ordered c(4×4) BaO structure is observed on the disordered sample surface.[26] Tan *et.al*,[27] also observed RT ferromagnetism in N-doped $BaTiO_3$ and the

origin of the magnetism was correlated with the presence of N. Therefore, studying the electronic properties of BaO is of great importance for devising new applications, specially in the area of magnetism. Hence, we propose to add a new functionality, i.e. magnetism, in BaO. We show that N in BaO has a ferromagnetic (FM) ground state and the transition temperature T_C, which is the temperature at which a material goes from a paramagnetic(disorder phase)state to a magnetic phase(order phase) state, is above the room temperature.

II. COMPUTATIONAL METHODS

To study the magnetism of N-doped BaO, we performed calculations in the framework of density functional theory, [28] using linear combination of atomic orbital basis as implemented in the SIESTA code [29]. A double-ζ polarized basis set for all atoms was used. The local spin density approximation[30](LSDA) was adopted for describing exchange-correlation interactions. We used standard norm-conserving pseudopotentials [31] in their fully nonlocal form [32]. A cutoff energy of 400 Ry for the real-space grid was adopted. The sampling of k-space was performed with Monkhorst and Pack (MP) scheme with a regularly spaced mesh of $18 \times 18 \times 18$. Convergence with respect to k-point sampling and cutoff energy was carefully checked.

To investigate the magnetism and electronic structures of N-doped BaO, we considered the $2\times2\times1$ ($Ba_4O_3N_1$), $2\times2\times2$ ($Ba_8O_7N_1$), $2\times2\times3$($Ba_{12}O_{11}N_1$) supercells of the primitive unit cell of NaCl-type BaO. Calculations were also carried out using a $3\times3\times3$ ($Ba_{27}O_{26}N_1$) supercell. In all these supercells, N was doped at O site due to smaller difference in their atomic sizes and electro-negativities. For the magnetic properties of BaO (001)surface, we considered the conventional unit cell of BaO, and used different $n \times m \times z$ symmetric slabs of thickness z, which is defined as a monolayer of BaO. We investigated $n = 1, m = 1, z = 8$ ($Surf_1$) and $n = 2, m = 1, z = 8$ ($Surf_2$) surfaces of BaO and doped N at O on both sides of the BaO surface. We added a vacuum region of about $\sim$ 10 Å, so that the two surfaces do not interact with each other through the vacuum region. Additional simulations, using plane waves plus pseudopotentials as implemented in the Quantum Espresso (QE) code[36], were also carried out to further test the validity of our results. Atomic positions were relaxed, using conjugate-gradient algorithm,[33] until the residual Hellmann-Feynman force on single atom converges to less then 0.05 eV/Å. Test calculations, using LSDA+U, were also carried

out by considering the on-site Coulomb correction (U = 6.0 eV, our previously optimized value[20]) between the p-orbital electrons of O.[20,34,35]

III. RESULTS AND DISCUSSIONS

First, we calculated the optimized lattice constant of NaCl-type BaO, and the optimized lattice constant is found to be 5.40Å , as shown in Fig. 1(a). The calculated lattice constant is comparable with the previous calculated 5.47Å,[37] and experimental 5.52Å[38] values. Our DFT estimated value is smaller than the experimental value due to the underestimation problem of DFT-LDA. Using the optimized lattice constant, we calculated the band structure, which is shown in Fig. 1(b). We see that BaO is a wide bandgap semiconductor and the calculated bandgap at the X point is $\sim$ 1.62 eV. The band is degenerate at G point $[2\pi/a(0,0,0)]$, but this degeneracy is removed at X point where the band has less curvature (large effective mass) as compared with point G. The electronic density of states (DOS) shows that bands near the Fermi energy ($E_{\rm F}$) are mainly derived from the O p-orbitals [see Fig. 2(a)]. The LSDA calculated indirect (Γ-X)bandgap is $\sim$ 2.0 eV, in agreement with the previous LDA calculation.[39] However, the experimental and GW calculated value is 3.88 eV[39–41]. We then used LSDA+U, and our LSDA+U calculated bandgap is $\sim$ 3.6, which is comparable with the GW calculated and experimental values.

It is important to consider atomic relaxation in N-doped BaO. Usually, the doped impurity at the host site can either compress or elongate the bond length depending on the atomic size of the impurity atom. In some cases the impurity atom can also go to the interstitial site and can form a defect complex.[20] We, therefore, relaxed all the atomic coordinates of BaO:N and no significant changes in the atomic positions of N at O sites were found. To further confirm it, both $Ba_8O_7N_1$ and $Ba_{12}O_{11}N_1$ were considered, and calculated their optimized lattice constants, which are 5.40Å for both the systems [see Fig. 1(a)]. This lattice constant is approximately equal to our optimized lattice constant of pristine BaO, which shows that N can easily be doped at O site without any structural distortion.

Figure 2(a) shows the calculated total and atom projected (P) DOS of N-doped BaO in the non-magnetic state. For comparison purpose, the total PDOS of pristine BaO is also shown. We can clearly see that the DOS of doped and pristine BaO are the same in the conduction and valance bands. However, near the Fermi energy ($E_{\rm F}$) the DOS of the doped

system is drastically changed and is showing metallic behavior in contrast to pristine BaO, which is an insulator. The PDOS demonstrates that the main peak at the Fermi energy is mainly contributed by the p-orbitals of N. The N atom in BaO forms an impurity band in the bandgap of BaO. A small impurity-derived peak can also be seen at 2.0 eV just below E_{F}, and this peak hybridizes with the p-orbitals of O atoms. Therefore, the O and N atoms only hybridize near the Fermi energy. No significant changes in the PDOS of O can be seen when N is doped at O site except a small shoulder, derived by the N p-orbitals, near the Fermi energy. The calculated results show that the top of the valence band consists of N $2p$ electrons which is higher than O $2p$ electrons. The large DOS at the Fermi energy $D(E_F)$ in the N-doped BaO shows that there is an instability towards magnetism within the Stoner mean field theory of magnetism.[43] Within the Stoner model, which was mainly proposed for itinerant electron system, the large $D(E_F)$ can lead to a large Pauli susceptibility and this susceptibility is large enough for the band to split spontaneously, and magnetism in N-doped BaO can be expected.

To confirm that N-doped BaO can have magnetism within the Stoner mean field theory, we further carried out spin-polarized calculations. The spin-polarized electronic density of state of $Ba_4O_3N_1$ is shown in Fig.2(b). The total DOS clearly shows that N induces magnetism in BaO when doped at O site. The spin-polarized structure shows that the non-magnetic impurity band in the bandgap [see Fig.2(a)] is mainly contributed by the minority spins. Large exchange splitting at N site can also be seen, as expected in the Stoner mean field theory. For comparison, we also show the total DOS of pristine BaO and one can easily judge that the conduction band of $Ba_4O_3N_1$ in the spin-up state is identical to BaO. The $2p$ states of nitrogen are located at the top of the valence band, which are mainly derived from the anion p-states, resulting in the hybridization of electron wave functions of the $2p$ orbitals. The majority spin-states of nitrogen also hybridize with oxygen $2p$ states, promoting the the impurity band which connects to the top of the valence band. Such chemical process gives birth to a bandgap in the majority spins states. The minority spins on the other hand create an impurity band in the bandgap which includes E_{F}. As a result this impurity band is broadened having about 0.38 eV half-width, and the approximated exchange splitting is 0.80 eV. The majority spins are completely occupied and behaving just like an insulator, whereas the minority spins are partially occupied and have a metallic nature. Such electronic structure is the fingerprint of a half-metal ferromagnet,[44,45] which

has applications in the area of spin electronics. The total and local magnetic moments of $Ba_4O_3N_1$ were also calculated, and the calculated total magnetic moment is $1.0\,\mu_B$ per unit cell. The PDOS clearly shows that the magnetic moment is mainly contributed by the N p-orbitals and the local magnetic moment at the N site is $\sim 0.74\,\mu_B$. A small induced magnetic moment ($\sim 0.20\,\mu_B$) at the nearby O site is also observed. The PDOS of O shows some unoccupied minority spin states, which were occupied in the pristine BaO, suggesting that the holes induced by N also localized at the O p-orbitals. We repeated the same calculations by doping N at O site in $2 \times 2 \times 2$ and $2 \times 2 \times 3$ supercells, and interestingly we found half-metallic behavior in all these doped systems [see Fig. 2(d,e)] and the magnetic moments were mainly localized at the N site. This is also noticeable that N does not polarize the whole valance band, it polarizes only the valance electronic states near the Fermi energy. Such behavior of N in BaO is different from transition metals in oxides/semiconductors which usually polarize the whole valance band.[46] The band-width of the N is decreased and the band is narrowed, as the concentration of N is reduced in BaO [see Fig. 2(e)], which further increases the localization of $2p$ states of N. This localization of the N $2p$ states may further increase the observance/suppression of ferromagnetism/antiferromagnetism in BaO, which is discussed in the following paragraph. The total magnetic moment per N atom is $1.0\,\mu_B$, which is indicating that the total magnetic moment is independent of the N concentrations. In all these N-doped BaO systems, the calculated magnetic moment is consistent with Hund's rules indicating that the N dopant exists as a N^{2-} (s^2p^5) anion illustrating that each N impurity introduces one $2p$ hole and the strong Hund-type exchange makes the nitrogen $2p$ spin-up orbitals completely occupied, and the spin-down states are partially filled [Fig.2(b-e)]. As a result, one can expect the (ferro)magnetism in N-doped BaO to be stabilized mainly by the predominant double-exchange mechanism.[43] Before we address the question of FM or antiferromagnetic (AFM) coupling between the N atoms, the above calculations were also performed for $Ba_{27}O_{26}N_1$ and $Ba_{32}O_{31}N_1$, and we confirmed that N in BaO has spin-polarized band structure. We also confirmed the above conclusions using the QE code.This is also important to comment on the magnetism of N-doped BaO using LSDA+U. The LSDA+U calculated total and PDOS of $Ba_4O_3N_1$ are shown in Fig. 2(c). As expected, the N forms an impurity band in the bandgap of BaO and N-driven oxygen p states can also be seen in the gap region of BaO. Similar observations were also observed in self-interaction correction (SIC) for C-doped BaO.[47] The local magnetic moment of N (O)is

increased (decreased), but the total magnetic moment of the unit cell remains unchanged, i.e., 1.0μ_B. Similar conclusions were also drawn when LSDA+U calculations were performed for $Ba_8O_7N_1$, and $Ba_{12}O_{11}N_1$ consistent with our previous work.[20]

As predicted that N can induce half-metallic magnetism in insulating BaO. However, there remains a question that whether N-doped BaO can have FM order above room temperature, and are the exchange coupling sufficiently large that can give rise to possible RT ferromagnetism. Magnetism is a cooperative phenomenon and a single N in BaO can not determine the true magnetic ground state. Therefore, we consider $2 \times 2 \times 3$ and $3 \times 3 \times 3$ supercells of BaO and doped two N atoms at different O sites. The distance between the two N atoms d was varied and considered the FM and AFM coupling between them. For comparison purposes, we keep the same N-N separation in both the supercells, and the results are summarized in Table I. This is enchanting to see that both BaO:N systems have FM ground state, and the total magnetic moment of the unit cell is 2.0 μ_B (i.e., 1.0 μ_B per N). All the systems remained half-metallic as well. The strength of the exchange interactions J can be judged from $\Delta E = E_{AFM} - E_{FM}$, where $E_{AFM}(E_{FM})$ is the total energy of the supercell in the AFM (FM) state. This exchange energy can be further used to estimate T_C. Using the Heisenberg mean field model ($k_B T_C = 2\,\Delta\, E/3$),[48,49] the estimated T_C is found to be close to room temperature proposing the possibility of room temperature ferromagnetism in BaO:N systems. One can also see that both the systems have different transition temperatures due to different N concentrations in BaO. Note that usually mean field theory overestimates T_C, but it can give an indication of possible RT FM. Therefore, RT ferromagnetism in N-doped BaO is expected, if properly prepared. It is encouraging to mention that our estimated T_C is matching with N-doped $BaTiO_3$[27] and other magnetic oxides[9,21] indicating that the magnetism is mainly contributed by N impurities.

The formation enthalpy H_f of BaO is calculated using $H_f = E(\mathrm{BaO}) - [\mathrm{E(Ba)} + \frac{1}{2}\mathrm{E(O_2)}]$, where E(BaO), E(Ba), and $E(O_2)$ are the total energies of NaCl-type BaO, BCC Ba, and oxygen molecule, respectively. The calculated H_f is found to be -6.49 eV, which comparable with the previous calculated (-5.64[37], -5.19[50]), and experimental (-5.74[51]) values. We followed our previous approach[20] and calculated the defect formation energy E_f of N in BaO under Ba-rich and O-rich conditions because the defect formation energy strongly depends on the growth condition and chemical potential.[20] The calculated E_f of $Ba_4O_3N_1$, $Ba_8O_7N_1$, and $Ba_{12}O_{11}N_1$ in Ba-rich (O-rich) conditions are -1.15 (5.33), -1.14 (5.34), and -

1.15 (5.45) eV, respectively. This is clear to see that N in BaO has a negative defect formation energy under Ba-rich condition, which further increases the possibility of N in BaO. Note that LSDA+U calculated E_f of $Ba_4O_3N_1$ is about 6.6 eV in O-rich condition, which is increased by including U parameter–similar behvior is also observed in other oxides.[20] We then varied the distance d between the two N atoms, using $2\times 2\times 3$ and $3\times 3\times 3$ supercells, and calculated E_f under different growth conditions. The calculated E_f per N atom of both the systems in the FM states are shown in Table I. The calculated E_f are in the range of a single N doped BaO, and therefore we can not expect clustering of N in BaO when doped at O site. The formation energy depends on the N concentrations in BaO. We may safely conclude that all the studied systems have negative formation energies under Ba-rich environments. Such calculated results can help experimentalists to dope N in BaO. The role of intrinsic defects (vacancies) can not be ignored when we synthesise a sample and these intrinsic defects may interact with the impurity atom, and such interaction may further decrease E_f of the impurity atom.[20] There is also an experimental report on N-induced ferromagnetism in $BaTiO_3$,[27] which suggests the possible doping of N at O site in BaO. Experimental work will be very helpful to further analyse the possibility of N in BaO.

To propose BaO for practical practical applications, e.g., in the area of thin films, it is very essential to study the electronic and magnetic properties of N doped at surface O site in BaO, $Surf_1$. We found that N can also induce magnetism in BaO (001) surface, and the magnetism is mainly localized at the N site as shown in Fig.3(a,b). Surface oxygen atoms have negligible magnetic moment and N has a large magnetic moment ($0.97\mu_B$) when doped at surface O site as expected for surface N atom. No induced magnetic moment at the subsurface atoms were found, which is different from other doped oxides.[1,52] The PDOS of surface O atoms are shifted towards the Fermi energy as compared with the clean surface O atom indicating that the band gap of BaO(001) surface is reduced due to surface states driven by N-O hybridization. The majority spins of N are occupied and the minority spins are partially occupied. The calculated surface spin densities of N, O, and Ba atoms are shown in Fig.3(c), and it is evident to see no spin-polarization at the surface O and Ba atoms. The spin density is mainly localized around the N atoms. We then used $n\times m\times z$ surface ($Surf_2$) and doped two N atoms at two different O sites and considered the FM and AFM coupling between the N atoms. Here we also found FM coupling between the surface N atoms has lower energy than the AFM coupling. As the concentration of N atom is increased,

a small magnetic moments at the surface O atoms were also induced, but the sub-surface O atoms did not show any induced magnetic moment[Fig.3(b)]. No surface relaxation or reconstruction was observed, when all the atoms were fully relaxed. The calculated E_f of N at surface O in Ba-rich (O-rich) condition is -1.58 (4.90) eV for $Surf_1$. For $Surf_2$, when the two N atoms were doped at the surface O sites, the E_f per N in Ba-rich (O-rich) condition is -1.48 (5.00) eV when the distance between the two surface N atom is 3.82Å, whereas when the separation between the two N atoms is 5.40Å, the calculated E_f per N in Ba-rich (O-rich) condition is -1.60 (4.88) eV. The surface N-doped BaO has a smaller defect formation energy than the bulk N-doped BaO, similar to other oxides.[52] Note that a smaller surface E_f corresponds to a larger N-N bond distance suggesting that N prefers isolation than clustering in BaO(001) surface.

We have shown that N in BaO can have possible room temperature ferromagnetism either in bulk or surface doped system, and finally we would like to compare it with the Co-doped BaO. Our preliminary results clearly indicate that a Co atom at either O or Ba site induces magnetism with a larger(about 3 times) E_f than BaO:N systems. Therefore, we have firm believe that N in BaO has the opportunity to easily tune magnetism and may be superior to Co doped BaO. Further experimental work would be needed to propose BaO:N for possible applications in the area of spin electronics. We also believe that our prediction can also be helpful for BaO terminated surface of $BaTiO_3$.

IV. SUMMARY

To summarize, DFT is used to investigate the possible magnetism in N-doped NaCl-type BaO. Pristine BaO is shown to be non-magnetic wide bandgap semiconductor, and N at O site induces an impurity band in the bandgap of BaO. It is discussed that N in BaO can also induce magnetism and the magnetism is mainly contributed by the N atoms. The minority impurity-driven band is narrowed with decreasing the N concentrations in BaO. The origin of magnetism was elucidated from the atom projected density of states. All the considered N concentrations in BaO showed half-metallic behavior. The ferromagnetic and antiferomagnetic interactions between the N atoms were also considered, and it revealed shown that N-doped BaO is a ferromagnetic material. The transition temperature was also calculated, using Heisenberg mean field model, which was above room temperature.

The magnetic interactions between the N atoms is limited to the next-nearest-neighbor interactions. The surface magnetism of N-doped BaO(001) was also studied by doping N at surface O site. N at surface O site also showed ferromagnetic ground state, and the magnetism was mainly limited to the BaO surface. No induced magnetic moments were observed at the sub-surface O sites. The defect formation energies showed that N has a smaller formation energy than the bulk N doped BaO. The magnetism of N-doped BaO was also compared with Co-doped BaO, and it was concluded N-doped BaO can easily be achieved. LSDA+U calculations also supported ferromagnetism in N-doped BaO.

The author acknowledges insightful discussions with Víctor M. García-Suárez and the cluster facilities of NCP, Pakistan.

* gulrahman@qau.edu.pk

[1] G. Rahman and V. M. García-Suárez, Appl. Phy. Lett. **96**, 052508 (2010).

[2] G. Rahman, V. M. García-Suárez, and J. M. Morbec, J. Magn. Magn. Mater. **328**, 104 (2013).

[3] Wen-H. Xie, Ya-Q. Xu, Bang-Gui Liu, and D. G. Pettifor, Phys. Rev. Lett. **91**, 037204 (2003).

[4] J. E. Pask, L. H. Yang, C. Y. Fong, W. E. Pickett, and S. Dag, Phys. Rev. B **67**, 224420 (2003).

[5] C. Wen Zhang, and S. shen Yan, Appl. Phys. Lett. **95**, 232108 (2009).

[6] M. Khalid, M. Ziese, A. Setzer, P. Esquinazi, M. Lorenz, H. Hochmuth, M. Grundmann, D. Spemann, T. Butz, G. Brauer, W. Anwand, G. Fischer, W. A. Adeagbo, W. Hergert, and A. Ernst, Phy. Rev. B **80**, 035331 (2009).

[7] D. Kim, J. Hong, Y. Ran Park and K. Joo Kim, J. Phys.: Condens. Matter **21**, 195405 (2009).

[8] J. B. Yi, C. C. Lim, G. Z. Xing, H. M. Fan, L. H. Van, S. L. Huang, K. S. Yang, X. L. Huang, X. B. Qin, B. Y. Wang, T. Wu, L. Wang, H. T. Zhang, X. Y. Gao, T. Liu, A. T. S. Wee, Y. P. Feng, and J. Ding, Phys. Rev. Lett. **104**, 137201 (2010).

[9] N. N. Bao, H. M. Fan, J. Ding, and J. B. Yi, Appl. Phys. Lett. **109**, 07C302 (2011).

[10] J. M. D. Coey, , M. Venkatesan, , C. B. Fitzgerald, Nat. Mater. **4**, 173 (2005).

[11] S. K. Srivastava, P. Lejay, B. Barbara, S. Pailhés, V. Madigou, and G. Bouzerar, Phys. Rev. B **82**, 193203 (2010).

[12] W. Zhi Xiao, L. Ling Wang, L. Xu, Q. Wan, and Zou, Solid State Communications **149**, 1304-1307 (2009).

[13] K. Sato and H. Katayama-Yoshida, Semicond. Sci. Technol. **17**, 367 (2002).

[14] G. Rahman, V. M. García-Suárez, and S. C. Hong, Phys. Rev. B **78**, 184404 (2008).

[15] W.-Z. Xiao, L.-L. Wang, L. Xu, Q. Wan, and B. S. Zou, Solid State Commun. **149**, 1304 (2009).

[16] W. Zhou, L. Liu, and P. Wu, J. Magn. Magn. Mater. **321**, 3356 (2009).

[17] H. Wang, Y. Yan, Y. S. Mohammed, X. Du, K. Li, and H. Jin, J. Magn. Magn. Mater. **321**, 337 (2009).

[18] X. L. Wang, Z. Zeng, and X. H. Zheng, J. Appl. Phys. **101**, 09H104 (2007).

[19] S.-J. Hu, S.-S. Yan, X.-X. Yao, Y.-X. Chen, G.-L. Liu, and L.-M. Mei, Phys. Rev. B **75**, 094412 (2007).

[20] G. Rahman, N. Ud Din, V. M. García-Suárez and Erjun Kan, Phy. Rev. B **87**, 205205 (2013).

[21] H. Pan, J. B. Yi, L. Shen, R. Q. Wu, J. H. Yang, J. Y. Lin, Y. P. Feng, J. Ding, L. H. Van, and J. H. Yin, Phys. Rev. Lett. **99**, 127201 (2007).

[22] J. M. D. Coey, M. Venkatesan, P. Stamenov, C. B. Fitzgerald, and L. S. Dorneles, Phy. Rev. B **72**, 024450 (2005).

[23] G. Bouzerar and T Ziman, Phys. Rev. Lett. **96**, 207602 (2006).

[24] N.W. Cant, M.J. Patterson, Catal. Today **73**, 271 (2003).

[25] S.T. Weir, Y.K. Vohra, A.L. Ruoff, Phys. Rev. B **33**, 4221 (1986).

[26] C.Wu, K. Kruska, M. R. Castell, Surface Science **618**, 9410 (2013).

[27] X. Tan, C. Chen, K. Jin, and B. Luo, Journal of Alloys and Compounds **509**, L311 (2011).

[28] P. Hohenberg and W. Kohn, Phys. Rev. **136**, B846 (1964).

[29] J. M. Soler et al J. Phys.Condens.: Matter **14**, 2745 (2002).

[30] J. P. Perdew and A. Zunger, Phys. Rev. B **23**, 5048 (1981).

[31] D. R. Hamann , M. Schlúter and C. Chiang, Phys. Rev. Lett. **43**, 1494 (1979).

[32] L. Kleinman and D. M. Bylander, Phys. Rev. Lett. **48**, 1425 (1982).

[33] W. H. Press, B. P. Flannery, S. A. Teukolsky, W. T. Vetterling, New Numerical Recipes, Cambridge University Press, New York, 1986.

[34] I. Nekrasov, M. Korotin, and V. Anisimov, arXiv: cond-mat/0009107v1.

[35] S.-G. Park, B. M.-Köpe,and Y. Nishi, Phys. Rev. B **82**, 115109 (2010).

[36] P. Giannozzi, S. Baroni, N. Bonini, M. Calandra, R. Car, C. Cavazzoni, D. Ceresoli, G. L. Chiarotti, M. Cococcioni, I. Dabo, A. Dal Corso, S. Fabris, G. Fratesi, S. de Gironcoli, R. Gebauer, U. Gerstmann, C. Gougoussis, A. Kokalj, M. Lazzeri, L. Martin-Samos, N. Marzari,

F. Mauri, R. Mazzarello, S. Paolini, A. Pasquarello, L. Paulatto, C. Sbraccia, S. Scandolo, G. Sclauzero, A. P. Seitsonen, A. Smogunov, P. Umari, R. M. Wentzcovitch, J.Phys.: Condens.Matter **21**, 395502 (2009).

[37] Z. Alahmed, and H. Fu, Phys. Rev. B **76**, 224101 (2007).

[38] V. Milman et al., Int. J. Quantum Chem. **77**, 895 (2000).

[39] T. Lv, D. Chen, and M. Huang, J. App. Phys. **100**, 086103 (2006)

[40] R. J. Zollweg, Phys. Rev. **111**, 113 (1958).

[41] G. A. Saum and E. B. Hensley, Phys. Rev. **113**, 1019 (1959).

[42] P K de Boer and R A de Groot, J. Phys.: Condens. Matter **10**, 10241 (1998).

[43] D. J. Kim, *New Perspectives in Magnetism of Metals* (Kluwer Academic, Dordrecht/Plenum, New York, 1999)

[44] R. A. de Groot, F. M. Mueller, P. G. van Engen, and K. H. J. Buschow, Phys. Rev. Lett. **50**, 2024 (1983).

[45] G. Rahman, Phys. Rev. B **81**, 134410 (2010).

[46] Y. Wang,R. Zhang, J. Li, L. Li, and S. Lin Nanoscale Research Letters **9**, 46 (2014).

[47] V. A. Dinh, M. Toyoda, K. Sato, and H. K.-Yoshida, J. Phys. Soc. Jpn. **75**, 093705 (2006).

[48] J. Kudrnovský, I. Turek, V. Drchal, F. Máca, P. Wein- berger, and P. Bruno, Phys. Rev. B **69**, 115208 (2004).

[49] F. Máca, J. Kudrnovský, V. Drchal, and G. Bouzerar, Appl. Phys. Lett. **92**, 212503 (2008).

[50] H. Moriwake, Int. J. Quantum Chem. **99**, 824 (2004).

[51] *CRC Handbook of Chemistry and Physics* (Taylor and Francis, Boca Raton, FL, 2007)

[52] N. Ud Din and G. Rahman, RSC Adv. **4** 29884 (2014).

TABLE I. Calculated total magnetic moment M (in μ_B), $\Delta E = E_{AFM} - E_{FM}$ per cell (in eV), transition temperature T_C (in K), and defect formation energy E_f per N (in eV) of N-doped BaO ($3 \times 3 \times 3$). Ba_{rich} and O_{rich} shows E_f under Ba-rich and O-rich conditions, respectively. The first column shows N–N separation d (in Å). Values in the bracket are for $2 \times 2 \times 3$ supercell.

d	M	ΔE	T_C	E_f	
				Ba_{rich}	O_{rich}
3.82	2.0(2.0)	0.064(0.077)	495(597)	-1.05(-1.07)	5.42(5.40)
6.61	2.0(2.0)	0.035(0.089)	271(689)	-1.02(-1.08)	5.45(5.40)

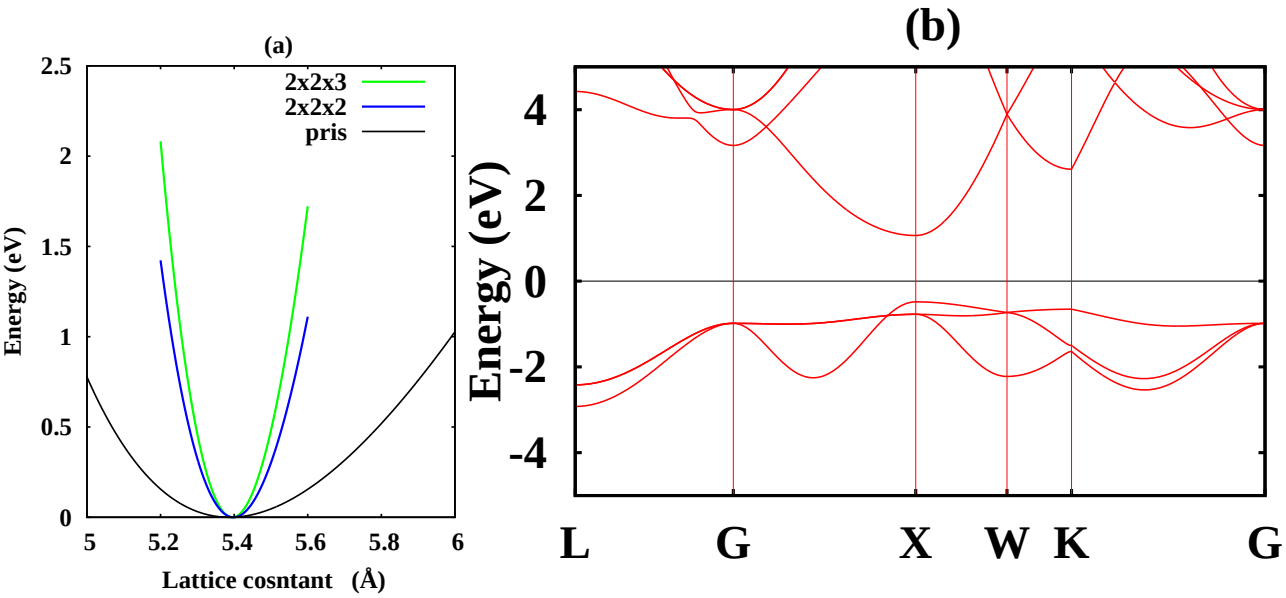

FIG. 1. (a) The calculated lattice constant vs energy of pristine BaO (black line), $Ba_8O_7N_1$ (blue line), and $Ba_{12}O_{11}N_1$(green line). (b) The band structure of pristine BaO, and the horizontal line (black) shows the Fermi energy, which is set to zero.

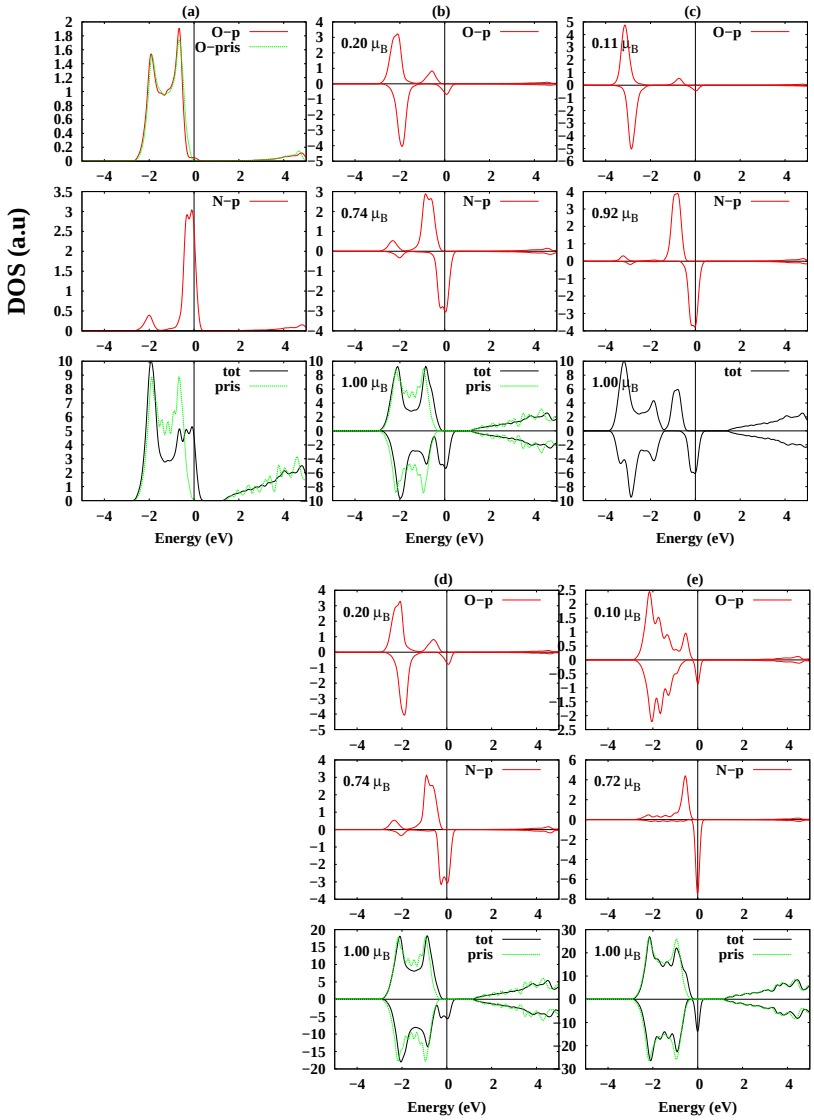

FIG. 2. The calculated total and atom projected density of states (PDOS) of $Ba_4O_3N_1$ in the non-magnetic (a), where the green dotted lines show the PDOS(O-pris) and total DOS (pris) of pristine BaO. The spin-polarized (magnetic) total and PDOS of $Ba_4O_3N_1$, $Ba_8O_7N_1$, and $Ba_{12}O_{11}N_1$ are shown in (b), (d), and (e), respectively. Panel (c) shows LSDA+U DOS of $Ba_4O_3N_1$. The green dotted lines in the total DOS panels show the total DOS of the pristine BaO (pris) of the same supercells. The total magnetic moments per N atom and local magnetic moments of N and O are also shown. The O and N PDOS are represented by solid (red) lines. The vertical lines show the Fermi energy, which is set to zero.

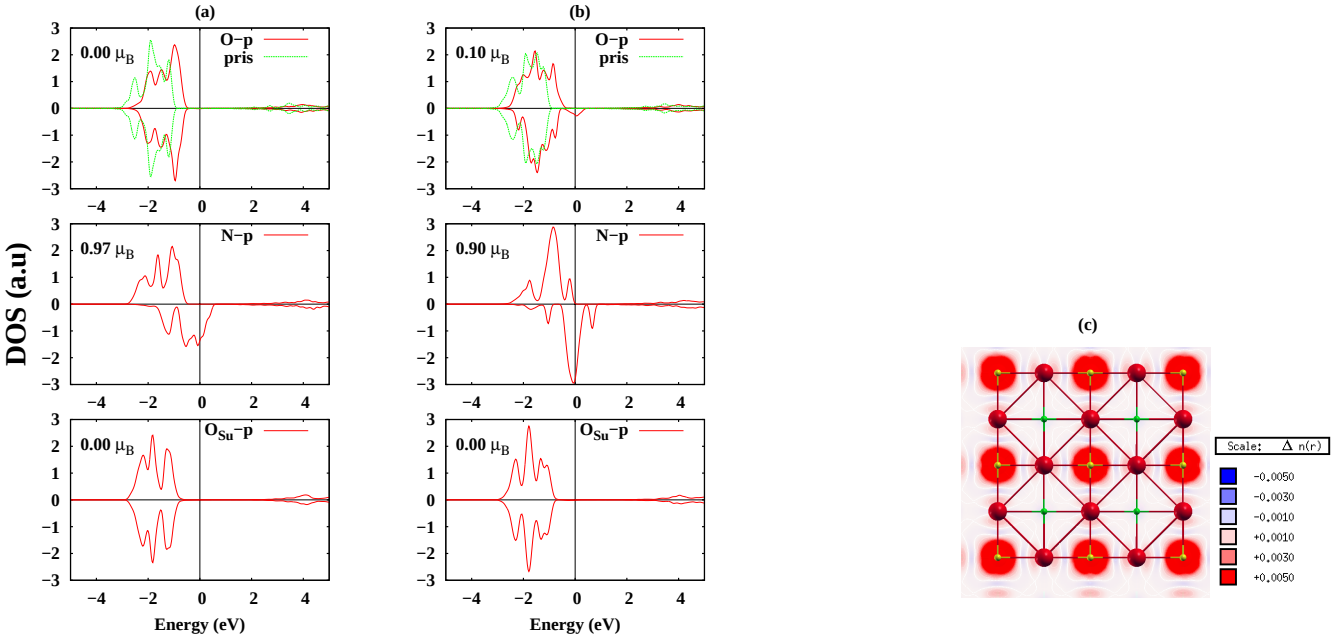

FIG. 3. The LSDA calculated surface atomic projected DOS of $Surf_1$(a) and $Surf_2$(b). The top panels show the PDOS of surface O atoms (red lines) along with the PDOS of clean surfaces O atoms (green lines). The middle panels show the PDOS of surface N atoms (red lines). The bottom panels shows the PDOS of sub-surface O atoms denoted as O_{Su}. The local magnetic moments of N and O atoms are also shown. The vertical lines show the Fermi energy, which is set to zero. The calculated surface spin density of $Surf_1$(c), where red, green, and yellow balls represent Ba, O, and N atoms, respectively. The spin density of $Surf_1$ is calculated on a large surface to show zero polarization at surface O atoms. The inset shows the scale of the spin density.